16th World Conference on Earthquake Engineering, 16WCEE 2017
Santiago Chile, January 9th to 13th 2017
Paper N° 5000 (Abstract ID)
Registration Code: S-S1477076523

GEER-ATC M_w7.8 ECUADOR 4/16/16 EARTHQUAKE RECONNAISSANCE PART I : SEISMOLOGICAL & GROUND MOTION ASPECTS

S. Nikolaou[1], X. Vera-Grunauer[2], R. Gilsanz[3], R. Luque[4], T. Kishida[5], G. Diaz-Fanas[6], N. Antonaki[7], T. Toulkeridis[8], E. Miranda[9], V. Diaz[10], D. Alzamora[11], A. Athanasopoulos-Zekkos[12], G. Lyvers[13], E. Morales[14], P. Lopez[15], K. Rollins[16], C. Wood[17], T. O'Rourke[18], S. Lopez[19]

[1] *Principal, Multi-Hazards & Geotechnical Engineering, WSP|Parsons Brinckerhoff, nikolaous@pbworld.com*
[2] *Head of the Engineering Research Institute, Instituto de Ingeniería, Universidad Católica Santiago de Guayaquil, Geoestudios, Ecuador, xvg@geoestudios.com.ec*
[3] *Founding Partner, Structural Engineer, Gilsanz Murray Steficek LLP, USA, ramon.gilsanz@gmsllp.com*
[4] *PhD Candidate, University of California, Berkeley, obluque@gmail.com*
[5] *Assistant Project Scientist and Post-doctoral researcher, Pacific Earthquake Engineering Research (PEER) Center, University of California, Berkeley, tkishida@berkeley.edu*
[6] *Geotechnical Engineer, WSP|Parsons Brinckerhoff, diazfanasg@pbworld.com*
[7] *Geotechnical Engineer, WSP|Parsons Brinckerhoff, antonakin@pbworld.com*
[8] *Professor and Researcher of Geology, Geochemistry, Volcanology, Escuela Politecnica del Ejercito, & Univ. de las Fuerzas Armadas, EC, theofilost@usfq.edu.ec*
[9] *Professor, Associate Department Chair, Stanford University, USA, emiranda@stanford.edu*
[10] *Senior Structural Engineer, Gilsanz Murray Steficek LLP, USA, virginia.diaz@gmsllp.com*
[11] *Geotechnical Engineer, Federal Highway Administration, USA, daniel.alzamora@dot.gov*
[12] *Associate Professor, UMICHIGAN, USA, addazekk@umich.edu*
[13] *Structural Engineer, Army Corp of Engineers, USA, gabriela.m.lyvers@usace.army.mil*
[14] *PhD Candidate, Univ. at Buffalo & L. Colonel of EC Army Corps of Engineers, enriquea@buffalo.edu*
[15] *Professional Foundation Engineer, New York, USA, geostructeng@aol.com*
[16] *Professor, Brigham Young University, USA, rollinsk@byu.edu*
[17] *Assistant Professor, Univ. of Arkansas, USA, cmwood@uark.edu*
[18] *Thomas R. Briggs Professor, Cornell University, USA, tdo1@cornell.edu*
[19] *Geotechnical Engineer, Geoestudios, Ecuador, slopez@geoestudios.com.ec*

Abstract

On the evening of April 16th, 2016, a moment magnitude M_w7.8 earthquake struck northern Ecuador, offshore of its west coast. The earthquake was named Muisne after the city of its epicenter, located about 29 km south-southeast of the town of Muisne, in the province of Manabí, at a hypocentral depth of 21 km. In the first 24 hours, over 135 aftershocks were recorded with hundreds more in the weeks that followed. Overall, this earthquake and its aftershocks led to hundreds of fatalities, thousands of injuries, tens of thousands homeless and an economic impact estimated at 3% of the nation's Gross Domestic Product (GDP). This paper is the first part of two papers that will present selected geotechnical reconnaissance observations from this earthquake, including seismological and strong ground motion aspects, based on the reconnaissance findings from the mission of the team deployed by the Geotechnical Extreme Event Reconnaissance (GEER) Association and the Applied Technology Council (ATC) with a detailed report available at www.geerassociation.org.

Keywords: earthquake reconnaissance; geotechnical observations; strong ground motions; GEER; ATC.

1. Introduction

The main M_w7.8 earthquake hit Ecuador on April 16th, 2016, centered offshore of the west coast of northern Ecuador, followed by many aftershocks. Based on the United States Geological Survey (USGS), the main event was caused by shallow thrust faulting on or near the plate boundary between the Nazca and South America plates, where the Nazca subducts beneath the South America plate at a rate of 61 mm/yr. Subduction along the Ecuador and the Peru-Chile trenches farther south has led to uplift of the Andes mountains and has produced some of the largest known earthquakes, including the largest ever recorded M9.5 Chile earthquake in 1960.

The event drew the attention of the Geotechnical Extreme Events Reconnaissance (GEER) Association, due to the several hundred casualties, tens of thousands homeless, and destruction along the west coast, with evidence of severe ground shaking and geotechnical failures. GEER had activated a reconnaissance team with funding by the National Science Foundation (NSF) when a second major M_w6.1 event occurred on April 20th. The GEER team was joined by structural engineers funded by the Applied Technology Council (ATC). The US-based team was on the ground from April 26th to May 2nd, joined by Ecuadorian counterpart partners.

The GEER-Ecuador team was co-led by Dr. Sissy Nikolaou of WSP | Parsons Brinckerhoff (WSP|PB) from the US and Dr. Xavier Vera-Grunauer of the Universidad Católica de Santiago de Guayaquil and of the Geoestudios firm of Ecuador (EC). The NSF-funded GEER members that travelled to Ecuador were geotechnical engineers Mr. Daniel Alzamora (Federal Highway Administration), Prof. Adda Athanasopoulos-Zekkos (Univ. of Michigan), Ms. Gabriela Martinez Lyvers (US Army Corp of Engineers), Prof. Kyle Rollins (Brigham Young Univ.), and Prof. Clint Wood (Univ. of Arkansas). The US team members funded by ATC were structural engineers Mr. Ramon Gilsanz of Gilsanz Murray Steficek (GMS) and Ms. Virginia Diaz (GMS), who was the ATC recorder for the report preparation.

The GEER-ATC group joined other US team members, already in Ecuador, funded individually or by their institutions, including Prof. Eduardo Miranda (Stanford Univ.), Mr. Enrique Morales (Univ. at Buffalo; Lt. Colonel of EC Army Corps of Engineers), and Mr. Roberto Luque (Univ. of California at Berkeley). During the reconnaissance, Mr. Guillermo Diaz-Fanas (WSP|PB) served as GEER-Ecuador recorder for the information gathered and the US contact person along with Mr. Pablo Lopez (PE) who facilitated communications while aboard. The GEER-ATC USA team was joined by Ecuadorian partners from the government, army, universities, and private engineering firms and by a Colombian partner from Universidad Norte, Prof. Carlos Arteta. The Ecuador-USA GEER-ATC team met daily to discuss findings and plan the following days.

This paper is the first of two papers in this conference that will briefly summarize the seismic history of Ecuador and present some key seismological observations and strong ground motion records from the main M_w7.8 Muisne, Ecuador earthquake. More details can be found in [1] and [2].

2. Tectonic Setting and Historic Seismicity

The tectonic setting in Ecuador is unique, as it exhibits all forms of earth movements represented by three types of plate boundaries (divergent, convergent, and transform). Two divergent plate boundaries are present in the Pacific Ocean: the East Pacific Rise and Galapagos Spreading Center. In these areas, three distinctive oceanic crusts originate (Fig. 1): the Pacific, Cocos and Nazca oceanic plates (on a triple junction around the Galapagos microplate) which move away from each other at the same rate as fingernails grow. While these plates move away from each other, the Nazca Oceanic plate moves almost eastwards and collides along a convergent zone with the coast of the South American continent.

The South American continent itself is composed of two continental plates, the Caribbean and South American plates, neither of which move toward nor away from each other. Rather, they touch each other and move in opposite directions along the third type of plate boundary. This transformation or strike-slip fault, which extends from the Gulf of Guayaquil through Venezuela, is called the Guayaquil-Caracas mega-fault. Potential future earthquakes in Ecuador are anticipated along the Guayaquil-Caracas mega-fault, and as a result of the collision and subsequent subduction between Nazca oceanic and Caribbean/South American continental plates.

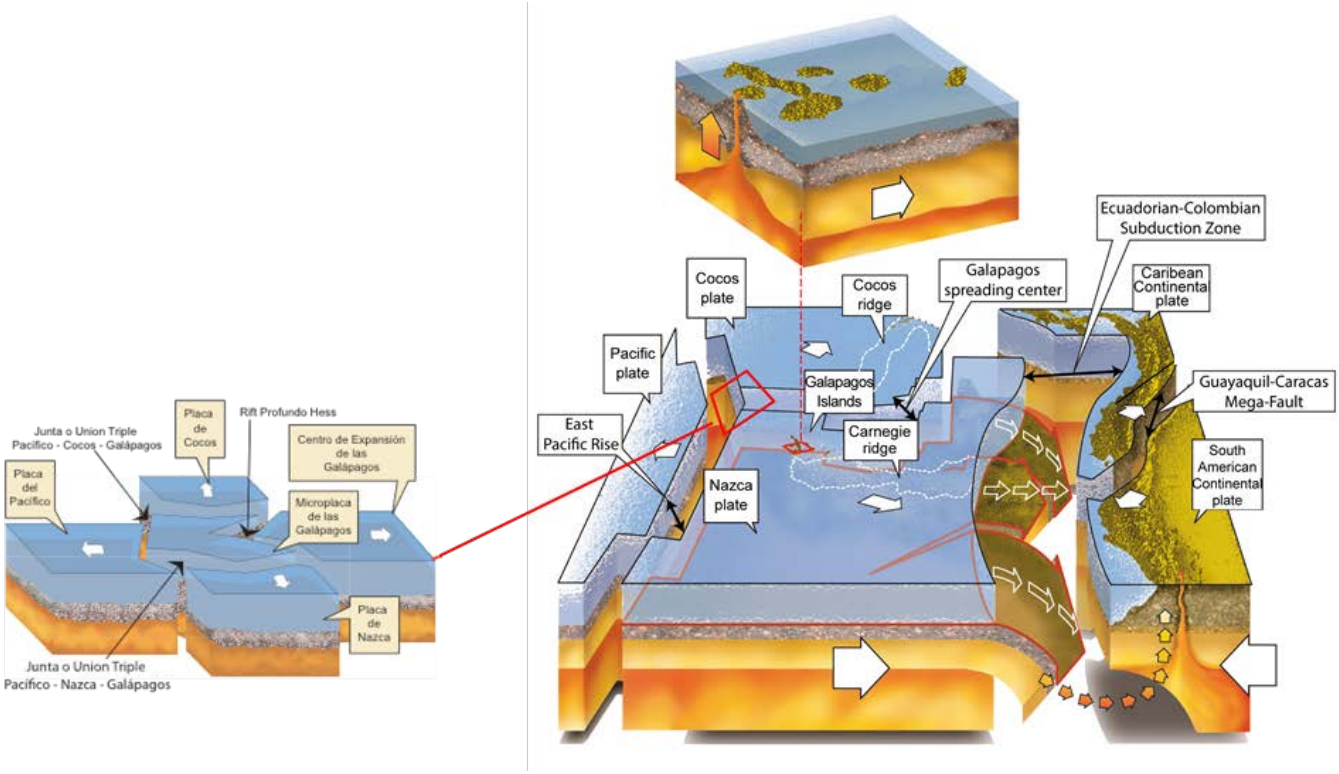

Fig. 1 – The geodynamic setting of Ecuador and associated plates, microplate and volcanic ridges (Oceanic Plates: Pacific, Nazca, Cocos; Continental Plates: Caribbean and South American; Oceanic Microplate: Galapagos, Ridges: Carnegie, Cocos (after [3]).

Ecuador has a long history of earthquakes, both of volcanic and tectonic (interplate and intraplate [4]) nature. According to Ecuador's Geophysical Institute, there have been at least 37 earthquakes of magnitude 7 or higher since 1541, when written records by the Spanish were first maintained. Fig. 2 (left) [5] summarizes events with minimum magnitude M of 4 from the unified earthquake catalog (1587–2009), and Fig. 2 (right) includes the 2016 events and highlights that the Ecuador – South Colombia subduction interface (between Lat. 0.5ºS and ~500 km north) has one of the highest seismic moment release rates in the world. The pink shaded area constitutes the aftershock zone for the 1998 M_w7.1 Bahía Earthquake Zone (BEZ).

In 1906, Ecuador was struck by a M_w8.8 megathrust earthquake near the city of Esmeraldas which ruptures a 500-km long area along the coast of Ecuador. The 1906 rupture area was subsequently "covered" by megathrust earthquakes in 1942, 1958, 1979 and 1998. However, Chlieh et al. [6] suggested that the potential for an event with $M_w > 7.5$ existed due to a seismic gap that had not been covered by the historic events after 1906, as depicted on Fig. 3.

The rupture area of the April 2016 M_w7.8 earthquake coincides with a portion of the Chlieh et al. [6] seismic gap. The zones of the 1942 and 2016 aftershocks border on, but do not overlap, the BEZ from Fig. 2 (right). The BEZ may have acted as a barrier for the southern propagation of the 1942 and 2016 ruptures and for the 1906 mega-event as well. It shows a characteristic behavior of one event of M~7 every 50-100 years and seems to behave independently of the northern megathrust. The 200-km wide Carnegie ridge constitutes a barrier for large earthquakes to propagate southwards, similarly to other bathymetric features along the South American subduction zone [7].

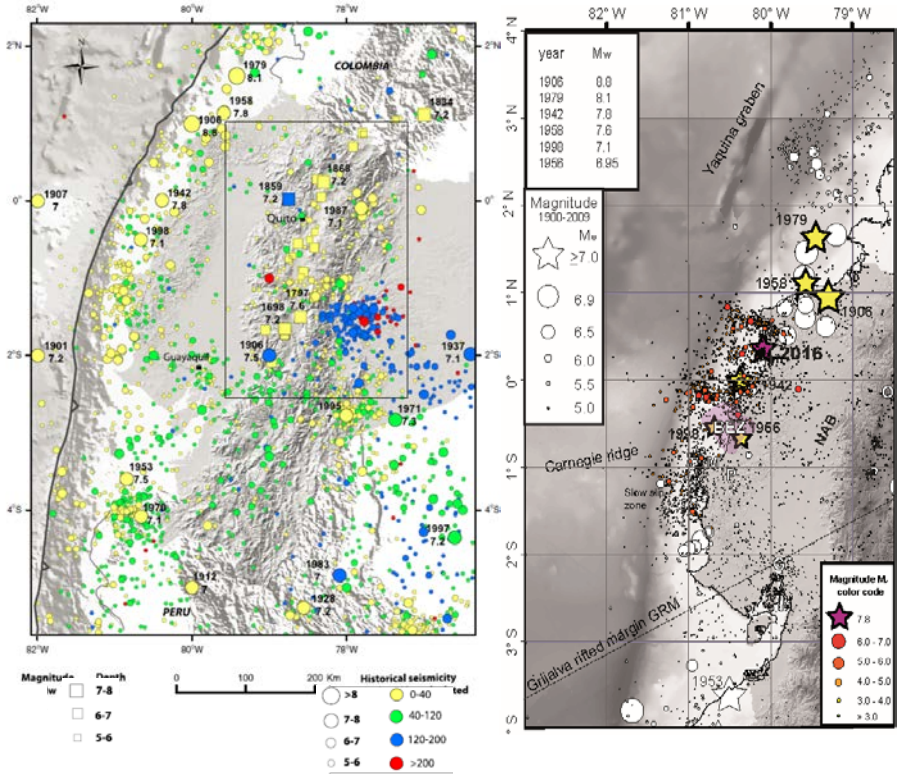

Fig. 2 – (Left) Epicenters from the unified earthquake catalog 1587–2009, integrating instrumental and historical earthquakes, Fig. 2 – (Left) Epicenters from the unified earthquake catalog 1587–2009, integrating instrumental and historical earthquakes, displaying magnitude 4 and above (after [4]). Historical seismicity equivalent M_w calculated from intensities (right). Epicenters of the main 2016 event (purple star) and its aftershocks (circles colored and sized according to magnitudes). Epicenters of historical earthquakes are shown in yellow stars and background seismicity prior to April 16th, 2016 are shown as black and white circles. (Base image: [5]).

3. Seismological Observations and Strong Ground Motions (4/16/16 Muisne Earthquake)

Fig. 2 (right) shows the epicenter of the 2016 earthquake as a purple star. Aftershocks and post-earthquake seismicity resulting from the 2016 M_w7.8 event are colored as shown in the lower right-hand corner. A summary of major aftershocks for 2016 earthquake is provided in Table 1.

Table 1 – Seismological parameters for major aftershocks of the 4/16/16 event [7].

DATE (mm/dd/yy)	UNIV TIME	LAT	LON	DEPTH (km)	MAGN M_w
04/17/16	21:35	0° 54' 36" S	80° 33' 36" W	10	6.5
04/20/16	8:35	0° 40' 48" N	80° 13' 12" W	4	6.3
04/22/16	3:03	0° 10' 48" S	80° 46' 12" W	10	6.2
05/18/16	7:57	0° 26' 24" N	79° 57' 0" W	7	6.6
05/18/16	16:46	0° 27' 36" N	79° 50' 24" W	9	6.7
07/11/16	2:01	0° 35' 24" N	79° 46' 12" W	10	6.2

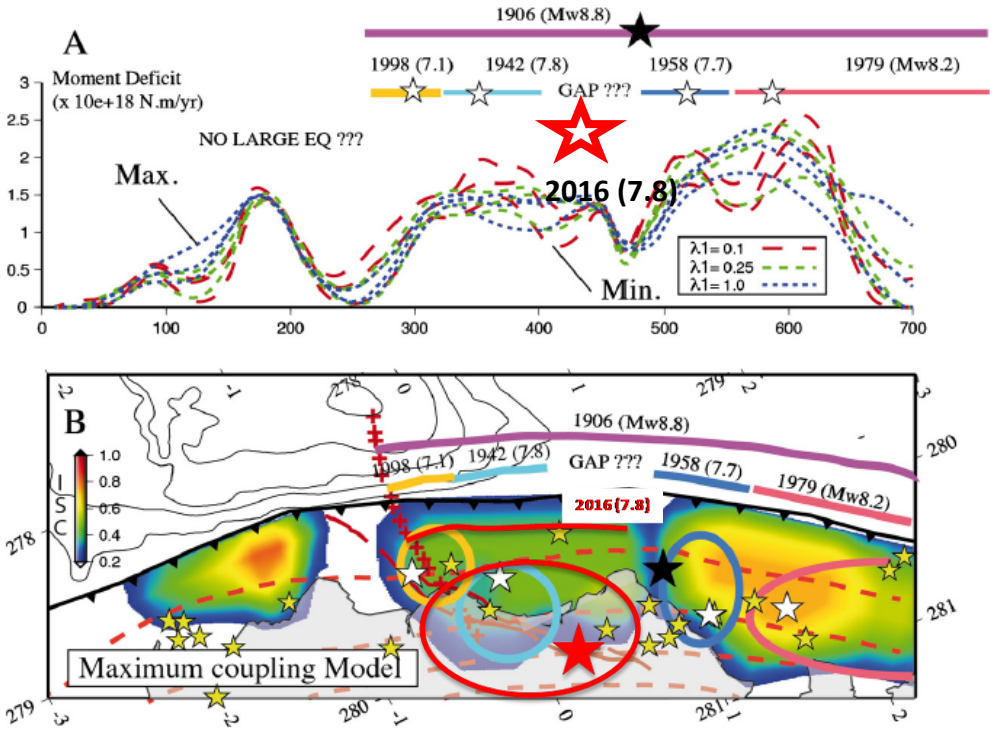

Fig. 3 – Historic seismicity of Ecuador and the seismic gap (modified from [6]).

Strong ground motion acceleration records [9] were provided to the GEER-ATC team by the Instituto Geofísico at the Escuela Politécnica Nacional (IG-EPN) which maintains and manages the National Accelerometer Network RENAC (Red Nacional de Acelerógrafos) throughout Ecuador. A total of 30 three-component uncorrected digital acceleration time series were provided from the main event from stations of RENAC, OCP (oil pipeline network) or LMI (a collaborative project between IG-EPN and the Institute of Research for Development, IRD, France). All records were processed except for one that was rejected due to the quality of the signal. Details on all instruments and stations are given in [1].

The records were processed by the GEER team following the PEER standard procedure [10], which includes inspection of record quality, selection of time windows, such as P-waves, S-waves, and coda waves, and component specific filter corner frequencies to optimize the usable frequency range. Table 2 presents details of 10 selected stations that recorded the main event with location (nearest city, latitude, longitude), closest distance to the rupture plane (R_{RUP}) using the USGS finite fault solution [11], recorded PGAs, and V_{s30} if available from [12], or directly measured by the Geoestudios firm during the GEER-ATC mission.

The strongest motion had a Peak Ground Acceleration PGA of 1.41 g was recorded in the EW component of the APED Pedernales station, with R_{RUP} of around 20 km, V_{s30} of 342 m/s, and with PGA of 0.83 g in the NS component. Another Pedernales station, PDNS (R_{RUP} = 21 km), recorded PGAs of 1.03 and 0.94 g in the EW and NS components. Fig. 4 shows EW acceleration time series for selected stations, overlying a map of Ecuador. Station AV21, near Esmeraldas has a smaller distance than station ACHN (25 *vs.* 34 km), but recorded half the amplitude of ACHN. Stations APED, PDNS, AMNT, ACHN and APO1 recorded PGA > 0.3 g. AGYE and AGY2 recorded significantly different PGAs (0.02 vs. 0.094g), as they are based on hard rock (V_{s30} = 1,800 m/s) and soft soil (V_{s30} = 101 m/s), respectively.

Long-period motions are generally better observed in terms time histories of velocities or displacements. A comparison of acceleration, velocity and displacement time histories for all stations can be found in [1].

Table 2 – Characteristics of stations with ground motion records processed by GEER using the PEER method.

Station	City	Geographic Coordinates		R_{RUP} (km)	V_{S30} (m/s)	PGA (g)		
		Latitude	Longitude			EW	NS	VER
PDNS	Pedernales	0° 6' 39.6" N	79° 59' 27.6" W	21	-	1.034	0.942	0.573
APED	Pedernales	0° 4' 4.8" N	80° 3' 25.2" W	20	342[a]	1.408	0.83	0.742
AES2	Esmeraldas	0° 59' 27.6" N	79° 38' 45.6" W	51	-	0.154	0.111	0.044
ACHN	Chone	0° 41' 52.8" S	80° 5' 2.4" W	34	200[a]	0.328	0.371	0.173
APO1	Portoviejo	1° 2' 16.8" S	80° 27' 36" W	73	224[a]	0.317	0.381	0.105
AMNT	Manta	0° 56' 27.6" S	80° 44' 6" W	76	496[a]	0.404	0.525	0.162
EPNL	Quito	0° 12' 43.2" S	78° 29' 31.2" W	104	-	0.027	0.02	0.013
AGYE	Guayaquil	2° 3' 14.4" S	79° 57' 7.2" W	155	1800[b]	0.019	0.024	0.015
AGY1	Guayaquil	2° 15' 3.6" S	79° 54' 36" W	175	178[b]	0.059	0.065	0.02
AGY2	Guayaquil	-2° 11' 56. 4" S	79° 53' 56.4" W	170	101[b]	0.094	0.098	0.038

[a] Measured by Geoestudios (2016). [b] Measured by Vera-Grunauer [12].

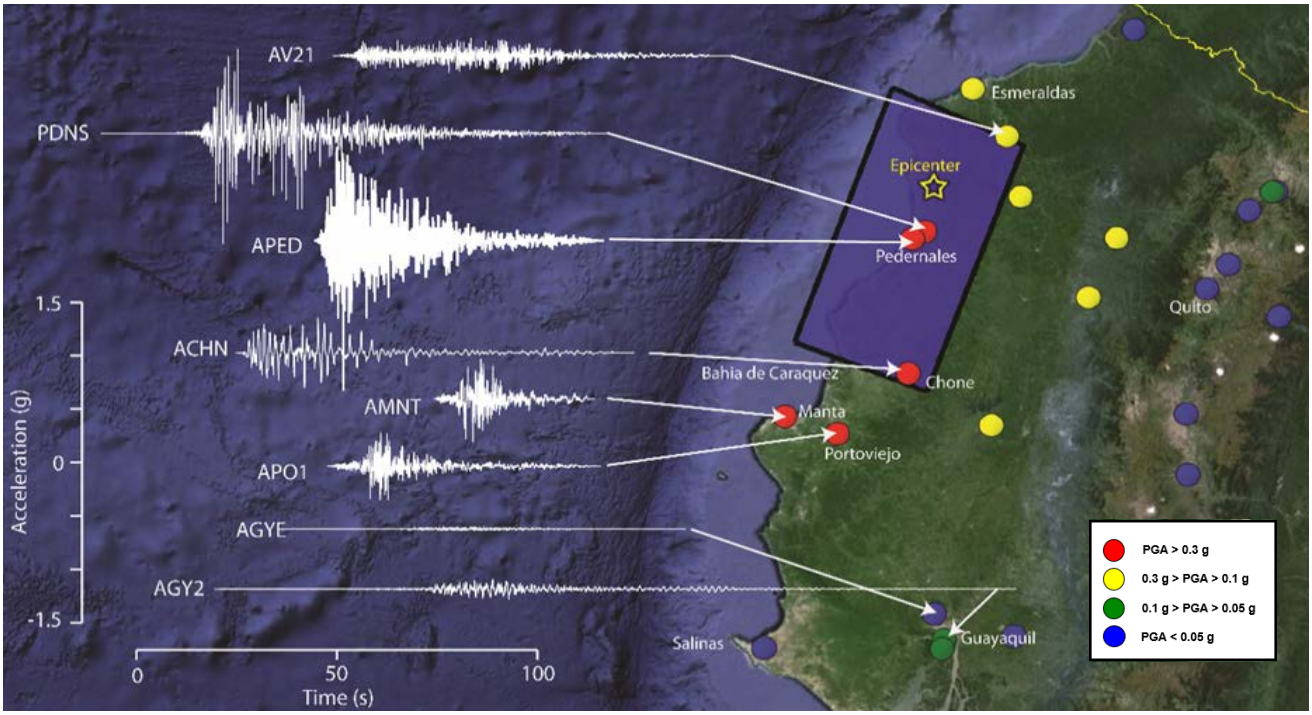

Fig. 4 – Acceleration time series in the EW component overlying a map of Ecuador with main cities and recording stations. Color-coded by the intensity of the motion in terms of the geo-mean Peak Ground Acceleration (PGA). For details, see [1].

Recorded strong ground motions were compared to predictions from the Ground Motion Prediction Equation (GMPE) BCHydro subduction model [13] with the parameters shown on Table 3. The closest distance to the rupture R_{RUP} was estimated using the USGS [11] finite fault model. An average shear wave velocity V_{s30} of 400 m/s was assumed for stations where V_s measurements were not available. The recorded PGA and Spectral Acceleration (SA) at structural periods T of 0.2, 1.0 and 3.0 s were compared to the median and ±σ of the GMPE values. The between-event residuals (δB) for these periods were also calculated.

Table 3. Parameters of the BCHydro subduction Ground Motion Prediction Equation [13].

PARAMETER	VALUE	COMMENTS
Magnitude, M_W	7.8	--
F_{type}	0	0 (interface), 1 (intra-slab)
F_{aba}	0	0 (force-arc), 1 (back-arc[1])
Flag_deltaC1	1	Period-dependent values of ΔC1
Period (T)	several	--
Distance to Rupture (R_{RUP})	see Table 5.2.1	USGS finite fault model
Hypocentral Distance (R_{hyp})	--	intra-slab events only
$V_{S,30}$	see Table 5.2.1	400 m/s if $V_{s,30}$ not known

Fig. 5 shows GMPEs and recorded geometric-mean SAs for each station along with the median curve for the main event adjusted by δB. Calculated between-event residuals were -0.54, -0.61, -0.105 and -0.035 (in natural log units) for PGA, SA(0.2 s), SA(1.0 s) and SA(3.0 s), respectively. For short T, the median recorded SA is closer to the median −σ of the GMPE, while for long T, this SA is close to medians of other subduction events. The δB for the 2016 earthquake is within expected values of between-event residuals. The within-event residuals (δWes) estimated and the standard deviation (φ) of the δWes for each period was within 0.8-1.12, which is greater than φ of 0.6 in the GMPE, possibly due to model assumptions and uncertainties (see detailed discussion in [1]).

Fig. 6 presents a comparison between the recorded 5%-damped geometric-mean SA and the predicted from the BCHydro GMPE median and median ±σ values for selected stations. In the highest intensity area of Pedernales, SA values from strong motion records in stations PDNS and APED are in agreement with median values for periods T longer than 1 s, but closer to the median +σ for T shorter than 1 s. AMNT records show higher SA than the median +σ throughout the entire range of periods. Based on the geometry of the slopes near the stations and the in-situ V_s measurements, the elevated SA in the short-period range (< 0.5 s) may be explained by site effects due to the presence of a thin, low-V_s surficial layer and deeper rock layer identified throughout the site.

Topographic effects were also considered but may not be the main cause of the higher than expected recorded motions because the waves propagated from north to south, traveling away from rather than into the 24-m tall, nearly vertical cliff 5 m away from AMNT [14]. Also, the orientation of the long axis of the slope (azimuth of 80º) would suggest topographic effects in the NS component, which is not supported by the recorded motions. At period T ~ 3 s, the AMNT, APO1 and ACHN records show a slight bump in spectral acceleration with SA values greater than the median +σ. These SA peaks at the three stations suggest possible directivity or path effects, which can be further investigated using aftershock records.

In the short period range, APO1 shows a significant SA peak at 0.5 s, with amplitude 5 times larger than the PGA and almost double the median +σ. ACHN also has a clear SA peak at 1.5 s with amplitude approximately 5 times larger than the PGA and well above the median +σ. Station AV21 has smaller R_{RUP} than ACHN, but shows less intensity with longer duration (close to median −σ). This trend is consistently observed between stations at the north (AMA1 and AV21) and south of the rupture plane (AMNT, ACHN and APO1). At Guayaquil, stations AGYE and AGY2, on rock and soft soil respectively, show clear differences in spectral

shapes. SA values at AGYE are similar to the GMPE median −σ, while SA at AGY2 is between the median and median +σ. The spectral shape at AGY2 does not show a clear peak, but rather has an entire zone of high SA values ~0.2 to 0.3 g for T between 0.3 and 2.0 s, which is likely an indication of soft soil site effects [12].

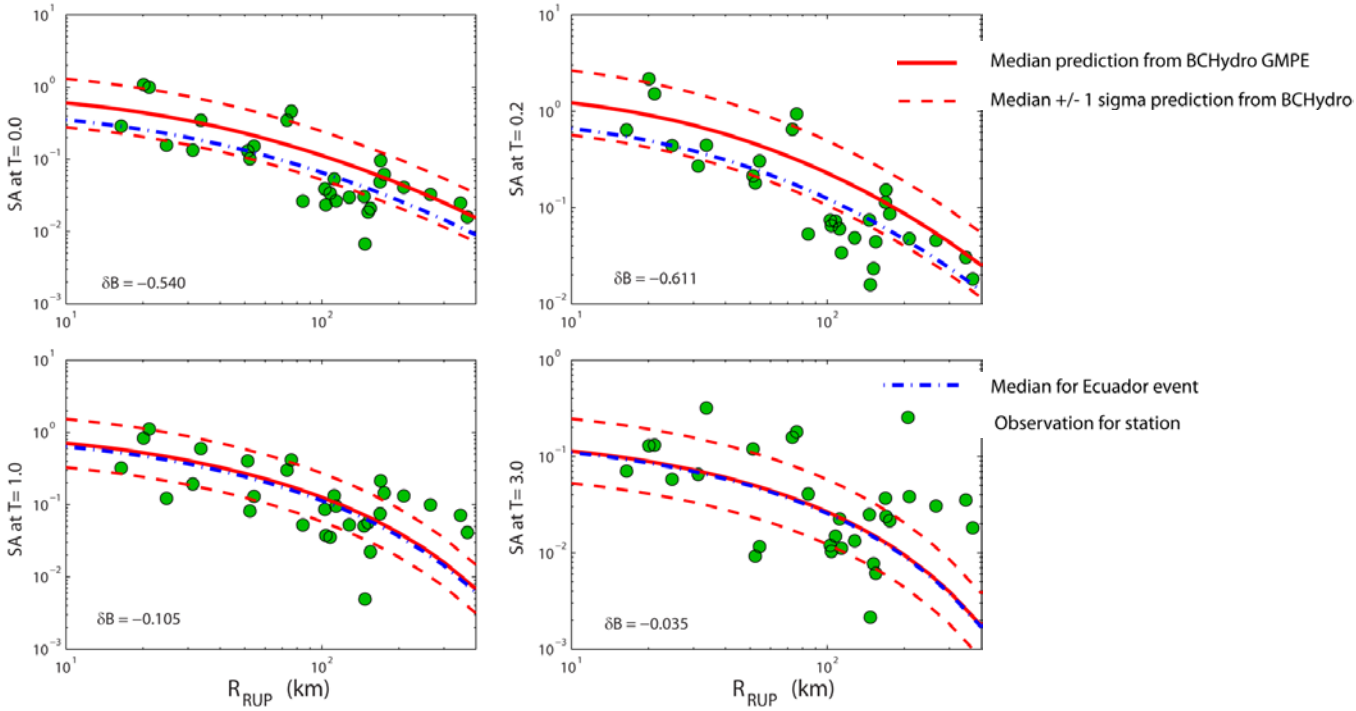

Fig. 5 – Observed ground motions (green dots), predicted by the BCHydro GMPE median (red solid line), median ±σ (red dashed line), and median curve for main Ecuador event (blue dashed line).

The Ecuadorian Construction Norm NEC-15 [15] in conjunction with ASCE 7-10 [16] was used to produce design spectra of the Maximum Considered Earthquake (MCE) with return period T_r of 475 years, for stations APED, PDNS, AMNT, APO1, ACHN, and AGY2. Table 4 shows the parameters used to derive the design spectra. The Z factor corresponds to PGA for the MCE for rock or stiff site conditions from NEC-15 [15]. Almost the entire coastline is mapped with Z = 0.5 g, which is a deterministic cap selected by code officials due to construction cost implications, since probabilistic PGAs were higher. Site amplification factors (F_a, F_d, F_s) were derived by classifying the site as per ASCE 7-10 [16] procedures using the V_{s30}. Other structural factors, such as η and r, were incorporated to produce the design acceleration spectrum.

Table 4. NEC-15 parameters for MCE design spectra for stations APED, PDNS, AMNT, APO1, ACHN, AGY2.

Station	Z	Site Class	V_{S30}	η	r	F_a	F_d	F_s
APED	0.5	D	342	1.8	1.0	1.12	1.11	1.40
PDNS	0.5	C	400	1.8	1.0	1.18	1.06	1.23
AMNT	0.5	C	496	1.8	1.0	1.18	1.06	1.23
APO1	0.5	D	224	1.8	1.0	1.18	1.11	1.40
ACHN	0.5	D	200	1.8	1.0	1.12	1.11	1.40
AGY2[1]	0.4	F	101	1.8	1.5	1.00	1.60	1.90

[1]Although this site is classified as "F", it will be compared site "E" NEC-15 design spectra for Guayaquil.

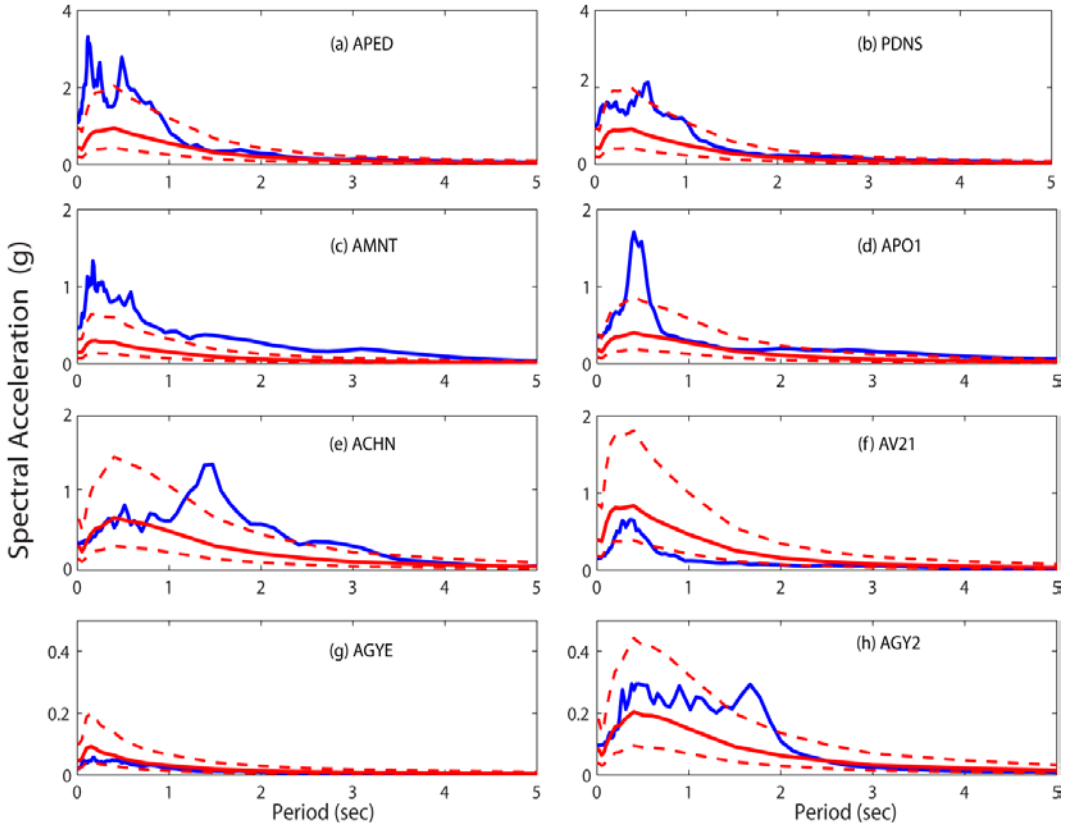

Fig. 6 –GMPE predicted 5% damped median and ±σ response spectra (red) and recorded geo-mean spectra (blue) for stations (a) APED, (b) PDNS, (c) AMNT, (d) APO1, (e) ACHN, (f) AV21, (g) AGYE, (h) AGY2.

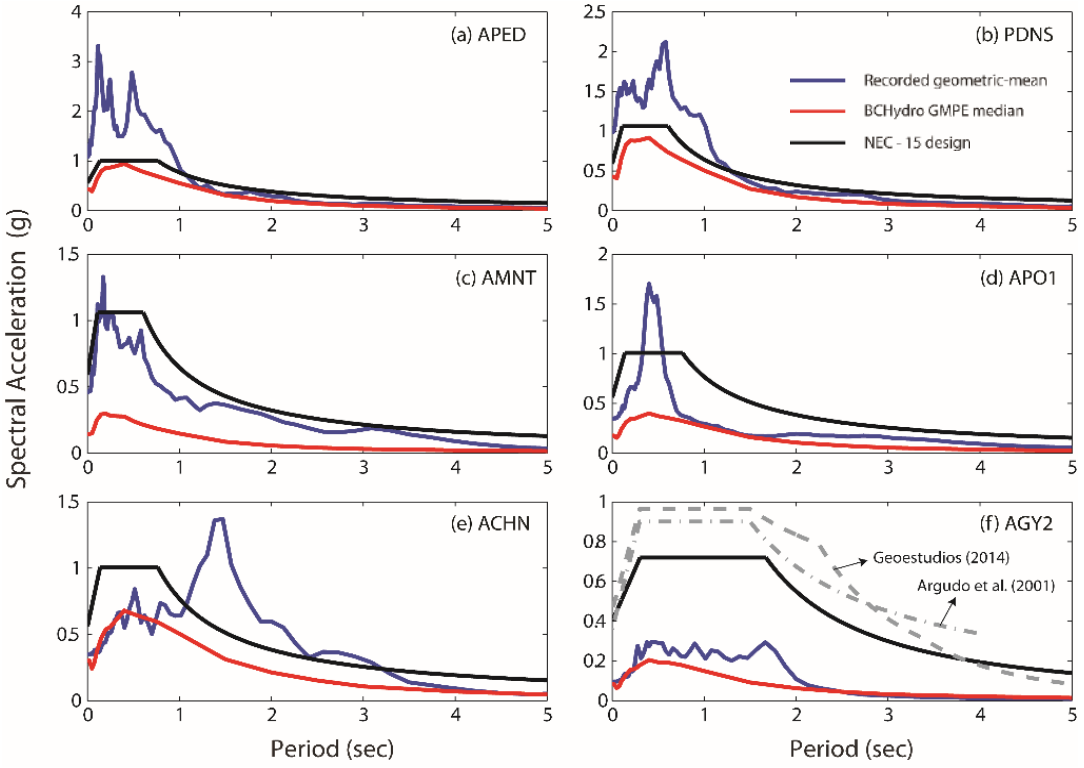

Fig. 7 – Comparison of recorded geometric-mean, median GMPE predictions, and NEC-15 design spectra for stations (a) APED, (b) PDNS, (c) AMNT, (d) APO1, (e) ACHN and (f) AGY2.

The MCE design spectra at the aforementioned stations, where V_{s30} data were available during preparation of the first version of the GEER-ATC report [1] are plotted on Fig. 7 and compared to recorded geomean response spectra and median GMPE predictions (Fig. 6). It is clear that the APED and PDNS (Fig. 7 a,b) recorded spectra are higher than the design spectra, while AMNT (Fig. 7 c), where site effects seemed to have played a part, is comparable to the NEC-15 spectrum. At APO1 (Fig. 7 d), the design spectrum is higher than the recorded spectrum with the exception of the peak of SA of 1.6 g around 0.5 s. ACHN (Fig. 7 e) shows recorded SA lower than design for T < 1 s, and higher between 1 and 2.5 s with a clear SA peak at ~1.5 s. The AGY2 (Fig. 7 f) SA are below design levels (assuming site class "E"), as well as site-specific studies in Guayaquil. Even though the SA amplitude varies, the spectral shape is similar to both the local code and the site-specific studies.

4. Conclusions

The unique tectonic setting of Ecuador has caused the country to have suffered through a long history of earthquakes of volcanic, as well as tectonic, both interplate and intraplate, nature. Six megathrust earthquakes with magnitudes over M7, including the most recent April 2016 Muisne earthquake, have occurred at subduction zones and generally within the same rupture area along the mega-earthquake of estimated magnitude of M8.8 along the Ecuadorian coast in 1906.

This paper is Part 1 of 2 in this conference that discusses selected observations from the GEER-ATC reconnaissance mission of the M_w7.8 April 16th, 2016 [1], focusing on seismological and strong ground motion aspects. The 2016 event produced several strong motion recordings, with PGA exceeding 1 g in the town of Pedernales. Seismic stations located towards the south of the rupture plane recorded larger shaking with shorter duration compared to the stations located towards the north, with similar closest distance to the rupture plane (R_{RUP}). Spectral acceleration data from 8 strong motion stations were compared to the median values derived using a subduction earthquake GMPE and the Ecuadorian Construction Norm (NEC-15). The values generally fell below the prediction at short periods and very close to it at longer periods. Six out of the eight recorded SA spectra were also compared to the design spectra and most records significantly surpassed the design values within different period ranges. Strong evidence of soil amplification in the amplitude and character of the response spectra was observed in most sites.

The second part of this paper will present selected geotechnical observations of the GEER-ATC reconnaissance mission [1], including liquefaction, settlements, and associated earthquake-induced effects in port structures and embankments.

5. Acknowledgements

The information contained in this paper is based on the GEER-049 report titled "GEER-ATC Earthquake Reconnaissance: April 16 2016, Muisne, Ecuador." This work was supported by the National Science Foundation through the Geotechnical Engineering Program under Grant No. CMMICMMI-1266418. The Geotechnical Extreme Events Reconnaissance GEER Association is made possible by the vision and support of the NSF Geotechnical Engineering Program Directors: Dr. Richard Fragaszy and the late Dr. Cliff Astill. GEER members donate their time, talent, and resources to collect time-sensitive field observations of the effects of extreme events. Financial contribution from the Applied Technology Council (ATC) funded the participation of two structural engineers in the mission. US agencies, academic institutions, and individuals volunteered with time and/or resources, all gratefully acknowledged in Chapter 3 of [1]. The engineering firms of WSP | Parsons Brinckerhoff (WSP|PB) and Gilsanz, Murray, Steficek, LLP (GMS) provided staff time and resources. Our colleagues in Ecuador were instrumental in providing local assistance and data, for which we are grateful and acknowledge in Chapter 3 of [1]. For this Part 1 paper, we would particularly like to acknowledge the Ministries of Urban Development & Housing (MIDUVI) and of Transportation & Public Works, the National Geophysical Institute, the 911 Emergency Response Agency, the Army Polytechnic School (ESPE) and the Army Corps of Engineers (ECACE).

6. References

[1] Nikolaou, S., Vera-Grunauer, X., and Gilsanz, R., eds., 2016. GEER-ATC Earthquake Reconnaissance: April 16 2016, Muisne, Ecuador, Geotechnical Extreme Events Reconnaissance Association Report GEER-049, Version 1. Authored by: Alvarado, A., Alzamora, D., Antonaki, N., Arteta, C., Athanasopoulos-Zekkos, A., Bassal, P., Caicedo, A., Casares, B., Davila, D., Diaz, V., Diaz-Fanas, G., Gilsanz, R., González, O., Hernandez, L., Kishida, T., Kokkali, P., López, P., Luque, R., Lyvers, G.M., Maalouf, S., Mezher, J., Miranda, E., Morales, E., Nikolaou, S., O'Rourke, T., Ochoa, I., O'Connor, J.S., Ripalda, F., Rodríguez, L.F., Rollins, K., Stavridis, A., Toulkeridis, T., Vaxevanis, E., Villagrán León, N., Vera-Grunauer, X., Wood, C., Yepes, H., Yepez, Y. Accessible at the GEER website geerassociation.org.

[2] Diaz-Fanas, G., Nikolaou, S., Vera-Grunauer, X., Gilsanz, R., Diaz, V., 2016. Selected Observations from the April 16, 2016 Muisne, Ecuador Earthquake, in 1st International Conference on Natural Hazards & Infrastructure (ICONHIC).

[3] Toulkeridis, T., 2013. Volcanes Activos Ecuador, Santa Rita, Quito, Ecuador: 152 pp.

[4] Schuster, R., Bolton, P., Comfort, L., Crespo, E., Nieto, A., Nyman, K., O'Rourke, T., 1991. The March 5, 1987, Ecuador earthquakes: Mass wasting and socioeconomic effects, National Academies Press, 184 pp.

[5] Beauval, C. et al., 2013. An earthquake catalog for seismic hazard assessment in Ecuador, Bulletin of Seismological Society of America, 103(2A):773-786.

[6] Chlieh, M., et al., 2014. Distribution of discrete seismic asperities and aseismic slip along the Ecuadorian megathrust. Earth & Planetary Science Letters, 400:292-301.

[7] Bilek, S.L., 2010. Seismicity along South American subduction zone: Review of large earthquakes, tsunamis, and subduction zone complexity, Tectonophysics, 495(1-2):2–14.

[8] Instituto Geofísico at the Escuela Politécnica Nacional, IG-EPN, 2016a. Acelerógrafos, Publicado en Instrumentación, igepn.edu.ec/acelerografos, last accessed 7/1/16.

[9] Singaucho J.C., Laurendeau A., Viracucha C., Ruiz M., 2016. Observaciones del sismo del 16 de Abril de 2016 de magnitud Mw7.8, Intensidades y Aceleraciones, Sometido a la Revista Politécnica.

[10] Ancheta, T., Darragh, R., Stewart, J., Seyhan, E., Silva, W., Chiou, B., Wooddell, K., Graves, R., Kottke, A., Boore, D., Kishida, T., Donahue, J., 2013. Pacific Earthquake Engineering Research, Report PEER 2013/03, PEER NGA-West2 Database.

[11] USGS, 2016. M7.8 Muisne, EC, Earthq. Hazards Program, United States Geologic Survey, earthquake.usgs.gov/earthquakes/eventpage/us20005j32#finite-fault, last accessed 5/18/16.

[12] Vera-Grunauer, X., 2014. Seismic Response of a Soft, High Plasticity, Diatomaceous Naturally Cemented Clay Deposit, Doctoral Dissertation, University of California, Berkeley.

[13] Abrahamson, N., Gregor, N., Addo, K., 2016. BC hydro ground motion prediction equations for subduction earthquakes, Earthquake Spectra, 32(1):23-44.

[14] Ashford, S.A., Sitar, N., 1997. Analysis of topographic amplification of inclined shear waves in a steep coastal bluff, Bulletin of Seismological Society of America, 87(3):692-700.

[15] NEC-15, 2015. Norma Ecuatoriana de la Construcción, Ministerio de Desarrollo Urbano y Vivienda, MIDUVI, Quito.

[16] ASCE 7-10, 2010. Minimum Design Loads for Buildings and Other Structures, American Society of Civil Engineers, Codes and Standards Committee